Research Article

SCI

Received: 15 October 2019 Revised: 19 December 2019 Accepted article published: 13 January 2020 Published online in Wiley Online Library: 21 February 2020

(wileyonlinelibrary.com) DOI 10.1002/jctb.6351

Kinetic evaluation of sterically hindered amines under partial oxy-combustion conditions

Sara Camino, Fernando Vega,* Luz M Gallego Fernández, Mercedes Cano, José A Camino and Benito Navarrete

Abstract

BACKGROUND: Carbon capture and storage is considered one of the pillars that should support greenhouse gas (GHG) emission mitigation by 2050. In this sense, partial oxy-combustion emerges as a promising alternative. Its advantages rely on the production of a higher CO_2 concentration flue gas than these provided by conventional air-firing processes. The use of higher CO_2 concentrations should improve the solvent kinetic and the CO_2 cyclic capacity.

RESULTS: The kinetic behaviour of two representative sterically hindered amines, namely 2-amino-2-methyl-1-propanol (AMP) and isophrondiamine (IF), were studied under partial oxy-combustion conditions in a laboratory-scale semi-batch reactor. The CO_2 concentration varied from 15%v/v to 60%v/v. The kinetic enhancement experienced by AMP at high CO_2 concentration was slightly >60%, instead of 70–80% for IF. AMP also improved its CO_2 absorption capacity by 24.7%, from 15%v/v to 60%v/v, almost doubled the improvements achieved by monoethanolamine (MEA). In the case of IF experiments, the CO_2 loading increased ≈10% from 15%v/v to 60%v/v CO_2 and it changed from 1.10 to 1.34 mol CO_2 mol^{-1} solvent, representing a >20% increase.

CONCLUSIONS: The presence of higher CO_2 concentrations accelerated CO_2 absorption and provided higher CO_2 absorption rates. In addition, the evolution of the CO_2 loading also exhibited higher values in the experiments using higher CO_2 concentration flue gas. The steric hindrance causes a hybrid behaviour in these solvents, between both fast and slow kinetic solvents. The kinetic rates observed using AMP were slightly higher than MEA, but lower than IF which showed the fastest kinetics.

Keywords: carbon capture; kinetics; clean processes; separation; emissions; pollution control

NOMENCLATURE

Chemicals

AMP, (–)	2-amino-2-methyl-1-propanol
IF, (–)	isophorondiamine
MEA, (–)	monoethanolamine

Symbols - Reactions

AmH (–)	Amine
AmH_2^+ (–)	Amine protonated
$AmCOO^-$ (–)	Carbamate
AmH^+COO^- (–)	Zwitterion intermediate
B (–)	Base
BH^+ (–)	Base protonated
CO_2 (–)	Carbon dioxide
H^+ (–)	Hydron
HCO_3^- (–)	Bicarbonate
H_2O (–)	Water
OH^- (–)	Hydroxide ion

Symbols – Equations

[AmH] (kmol m^{-3})	Amine concentration
[B] (kmol m^{-3})	Base concentration
$[CO_2]$ (kmol m^{-3})	Carbon dioxide concentration
$[CO_2]_{IN}$ (vol%)	Carbon dioxide inlet concentration
$[CO_2]_{OUT}$ (vol%)	Carbon dioxide outlet concentration
$[H_2O]$ (kmol m^{-3})	Water concentration
$[OH^-]$ (kmol m^{-3})	Hydroxide ion concentration
α (mol CO_2 mol^{-1} solvent)	CO_2 loading
α^* (mol CO_2 mol^{-1} solvent)	CO_2 loading at equilibrium
k_1 (m^3 kmol•s^{-1})	Forward reaction rate constant for CO_2 absorption reaction *via* zwitterion
k_{-1} (s^{-1})	Backward reaction rate constant for CO_2 absorption reaction *via* zwitterion
k_b (m^3 kmol•s^{-1})	Forward reaction rate constant for zwitterion hydrolysis reaction

* *Corresponding to: Fernando Vega, Chemical and Environmental Engineering Department, School of Engineering, University of Seville, C/ Camino de los Descubrimientos, s/n 41092 Sevilla, Spain. E-mail: fvega1@us.es*

Chemical and Environmental Engineering Department, School of Engineering, University of Seville, Sevilla, Spain

k_{H2} (m^3 kmol•s^{-1})	Forward reaction rate constant for bicarbonate formation (Eq. 8)
k_{OH-} (m^3 kmol•s^{-1})	Forward reaction rate constant for bicarbonate formation (Eq. 7)
Q_{fg} (mL min^{-1})	Flue gas flow-rate
r (kmol m^3•s^{-1})	Reaction rate
R (mL s^{-1})	CO_2 absorption rate
t (s)	Time
τ (s)	Characteristic time

INTRODUCTION

The European Commission has developed the 2030 climate and energy framework to contribute towards the Paris Agreement in order to keep global warming around 1.5 °C compared to pre-Industrial levels. The energy policies derived from this new energy scenario have been focused on moving to net-zero greenhouse gas (GHG) emissions and therefore towards a climate-neutral economy by 2050.[1] The portfolio of actions to mitigate GHG emissions consists of seven main strategies. Among them, carbon capture and storage (CCS) has a key role in contributing to the net-zero GHG emissions in the European Union by 2050, particularly to tackle the remaining CO_2 emissions after the implementation of the remaining strategies.[2]

In this context, the presence of CO_2 in the atmosphere has stablished above 400 ppm since 2014 although the efforts made on reducing GHG emissions worldwide.[3] According to the International Energy Agency (IEA), the CO_2 emissions increased by 1.65% in 2017 relative to the previous year and they reached up to 32.5 Gt CO_2.[4] In this sense, CCS technologies might contribute to mitigate CO_2 emissions directly from stationary sources and lead to a smooth transition towards deeper changes in the energy system. Post-combustion capture based on CO_2 chemical absorption is the most mature and closest-to-market CCS technology. However, the high operating costs and energy penalty associated with solvent regeneration constrain its deployment at large scales. Novel strategies such as partial oxy-combustion recently have been proposed to increase the CO_2 partial pressure in flue gas and, hence, to reduce the overall CO_2 capture cost.[5–7] The presence of higher CO_2 concentrations in flue gas showed benefits on the overall performance of the CO_2 capture process: enhancement of the CO_2 absorption kinetics,[8] reduction of the oxidative degradation rates[9,10] and decrease of reboiler duty.[7,11]

Novel solvents and blends have been proposed to reduce the energy requirements of the regeneration stage. High CO_2 absorption capacity, low volatility, low regeneration energy, stability to thermal and oxidative degradation are desired for a high-performance solvent for carbon capture.[12] The sterically hindered amines are prominent among the amine-based solvents. They were first studied by Sartori and Savage in gas-treatment applications.[13] They show an intermediate behaviour between primary and secondary amines: the presence of a large functional group close to the amino group produces weaker C—N bonds in the carbamate molecule after reacting with CO_2 and, therefore, the energy required for solvent regeneration is lower than both those provided by primary and secondary amines.

KINETIC AND REACTION MECHANISMS

The kinetics of sterically hindered amines differ significantly from primary and secondary amines. According to Zhang, the stability of carbamate ions formed by sterically hindered amines with CO_2 is significantly reduced.[14] The steric hindrance produces less stable carbamates during the absorption process compared to primary amines and enhances the formation of bicarbonates through reversion of carbamate, and thus the energy requirements for solvent regeneration decrease.[14] The CO_2 absorption enthalpy is ≈−80 kJ mol^{-1} CO_2.[15] The sterically hindered amines react with CO_2 following the zwitterion mechanism[16] [Eqn (1)]:

$$CO_2 + AmH \underset{K_1}{\leftrightarrow} AmH^+COO^- \quad (1)$$

The zwitterion intermediate undergoes a deprotonation process in the presence of a base, which can be another free amine in the aqueous solution, and produces the carbamate anion as occurs with primary and secondary amines [Eqn (2)]. The carbamate anion and the zwitterion intermediate show a similar low stability.

$$AmH^+COO^- + B \underset{K_b}{\leftrightarrow} AmCOO^- + BH^+ \quad (2)$$

Particularly for sterically hindered amines, the zwitterion intermediate also can undergo hydrolysis and produce bicarbonate, which is more stable [Eqn (3)]:

$$AmH^+COO^- + H_2O \rightarrow AmH_2^+ + HCO_3^- \quad (3)$$

However, the low stable carbamate derived from sterically hindered amines can be hydrolyzed to give bicarbonate [Eqn (4)] and free amines that may react readily with CO_2, as seen in the previous Eqn (1):

$$AmCOO^- + H_2O \underset{K_{OH}}{\leftrightarrow} AmH + HCO_3^- \quad (4)$$

In this case, the following reactions [Eqns (5)–(8)] occur simultaneously in the amine aqueous solution with fast kinetics, forming more bicarbonate, which is predominant over carbamate and zwitterion species in the solution:

$$AmH + H_2O \leftrightarrow AmH_2^+ + OH^- \quad (5)$$

$$H_2O \leftrightarrow H^+ + OH^- \quad (6)$$

$$CO_2 + OH^- \underset{K_{OH}}{\leftrightarrow} HCO_3^- \quad (7)$$

$$CO_2 + H_2O \underset{K_{H_2O}}{\leftrightarrow} HCO_3^- + H^+ \quad (8)$$

The resulting reaction rate for sterically hindered amines consists of the sum of the reactions where CO_2 forms bicarbonate, as shown in Eqn (9):

$$r = \frac{[CO_2][AmH]}{\frac{1}{k_1} + \frac{k_{-1}}{k_1 \sum k_b[B]}} + (k_{H_2O}[H_2O] + k_{OH^-}[OH^-])[CO_2] \quad (9)$$

In general, the sterically hindered amines have lower values of the reaction rate constant k_1 than those from primary amines,[17] of between 3600 and 13 000 m^3 $kmol^{-1}$ versus 810.4[16] and 740 m^3 $kmol^{-1}$ from 2-amino-2-methyl-1-propanol (AMP).[18] Due to the steric hindrance, these amines interact slowly with CO_2 to form weaker bonds with CO_2 in comparison with favoured kinetic amines, which are mainly primary and diamines.

The sterically hindered amine AMP is most used for CO_2 absorption applications, mainly blended with fast kinetic solvents that

promote the CO_2 absorption process. The CO_2 solubility of AMP and its blends have been determined in numerous studies performed using monoethanolamine (MEA),[19] diethanolamine (DEA),[20] piperazine (PZ)[20,21] and hexamethylenediamine (HMDA).[22] The use of AMP reduced the heat of absorption in comparison with a single amine in aqueous solution. According to Dash,[20,21] the CO_2 absorption enthalpy showed 15% decrease in AMP/PZ blends compared to PZ aqueous solutions. Recent studies from Wai[23] confirmed the high performance of AMP in combination with faster kinetic poliamines such as diethylenetriamine (DETA). Wai stated that the 2 mol L^{-1} AMP / 1 mol L^{-1} DETA blend provided the highest absorption performance for AMP/DETA blends. Other authors evaluated the behaviour of AMP blended with tertiary amines. Nwaoha studied the combination of AMP, PZ and MEA for CO_2 capture applications and demonstrated that the AMP/tertiary blends provided lower heat duty for solvent regeneration than conventional 5 mol L^{-1} MEA.[24]

In general, sterically hindered amines degrade less than primary amines. According to Wang and Jens, AMP showed lower thermal degradation rates in comparison with other primary amines such as MEA 5 M.[25] Therefore, the stripping temperature for AMP aqueous solutions should set in the range of 123–140 °C due to its high thermal stability whereas the stripping temperature for MEA aqueous solutions is normally fixed at 120 °C.[26] Respect to oxidative degradation, Vega *et al*. reported higher resistance to degradation of AMP blended with AEP (1-aminoethyl piperazine) at O_2 concentrations in the flue gas ≤6%v/v in comparison with 30 wt% MEA. In particular, MEA degradation was almost two-fold that of the AMP/AEP blend under port-combustion conditions (15%v/v CO_2) and 6%v/v O_2 in the flue gas.[10]

The sterically hindered amines can provide a springy behaviour for CO_2 capture based on chemical absorption and obtain further decrease of the energy requirement during solvent regeneration. Those springy solvents should exhibit a flexible kinetic behaviour between fast and slow solvents, showing elevated absorption rates with medium-to-low regeneration energies. In the present work, the absorption performance of this kind of amines was evaluated under partial oxy-combustion conditions and further compared with the benchmark (5 mol L^{-1} MEA). Two sterically hindered amines were studied, namely AMP and isophoronediamine (IF), using different CO_2 concentrations in flue gas from conventional post-combustion (15%v/v CO_2) up to 60%v/v CO_2.

MATERIALS AND METHODS

Materials

This work evaluated the absorption performance of two sterically hindered amines, namely AMP and IF, for further comparison with the benchmark 5 mol L^{-1} MEA. The amine-based solvents were supplied by Acros Organics™ (Geel, Belgium) with a purity of 99 vol% (Table 1). Deionized water was employed for the preparation of aqueous solutions of the different solvents tested in this work. The synthetic flue gas was prepared from pure CO_2 and N_2 gas cylinders supplied by Linde™. The supplier guaranteed a level of uncertainty in gas purity within ±1% as the certificate analysis (DIN EN ISO 6141) assessed. A 0.25 mmol L^{-1} phosphoric acid aqueous solution (supplied by Panreac™) was used in the CO_2 loading determinations with a level of uncertainty within ±1%. The concentration in aqueous solution of each solvent was selected following the optimization procedure described in detail in a previous work.[8]

Laboratory-scale apparatus

A detailed description of the laboratory-scale rig designed to afford the evaluation of CO_2 absorption performance has been summarized from previous works.[8] The laboratory-scale semi-batch rig (Fig. 1) consisted of a 250-mL reactor vessel immersed in a thermal-water bath, which adjusted the test temperature with an accuracy of ±0.1 °C. The reactor vessel was stirred at 300 rpm to avoid mass-transfer resistance during the test. The synthetic flue gas varied its composition from 15% v/v to 60% v/v CO_2, balanced with N_2. A 2 L min^{-1} flue gas was prepared using two mass-flow controllers which supplied the required CO_2 and N_2 flow rates from the gas cylinders. The synthetic flue gas was saturated in an impinger using deionized water and then injected into the reactor vessel in which the aqueous solution of the solvent had been introduced previously. The temperature of the pre-saturator also was controlled and maintained at the same temperature using the water-thermal bath. All of the experiments were set at 50 °C (conventional absorption temperature) and ambient pressure. The experimental procedure to perform the test campaign is described briefly as follows. Synthetic flue gas, provided by two mass-flow controllers adjusting the CO_2/N_2 mixture, was introduced into the reactor vessel where 220 mL of aqueous solution of the solvent to be tested was placed. The absorption of CO_2 occurred from the gas phase to the liquid phase, whereas the CO_2 loading of the liquid was gradually increased up to equilibrium. Then 1-mL liquid samples were withdrawn from the reactor vessel at different intervals during the test to determine the CO_2 loading achieved along the experimental time. After the CO_2 absorption occurred, the exhaust gas leaving the reactor vessel was cooled at the test temperature to avoid water loss and close the water mass balance. The CO_2 concentration of the exhaust gas was measured using a CO_2 Fourier transform infrared (FTIR) analyzer after cooling at 10 °C to remove the moisture of the exhaust gas. The test was finalized once the CO_2 concentration of the flue gas reached the starting value for each experiment.

Determinations

A pycnometer was used for kinematic viscosity determinations. Three measurements were performed for each amine aqueous solution tested in this work and the kinematic viscosity was determined from their main average value. The accuracy of the kinematic viscosity determinations were found within ±0.2 cP.

Table 1. Summary of the amine-based solvents studied in this work

Typology	Solvent	Abbreviation	Chemical Formula	Molecular Weight	CAS number	Concentration in aqueous solution (wt%)
Primary Amines	Monoethanolamine	MEA	C_2H_7NO	61.08	141–43-5	30
Sterically Hindered Amines	2-Amino-2-methyl-1-propanol	AMP	$C_4H_{11}NO$	89.14	124–68-5	20
	Isophorndiamine	IF	$C_{10}H_{22}N_2$	170.30	2855–13-2	40

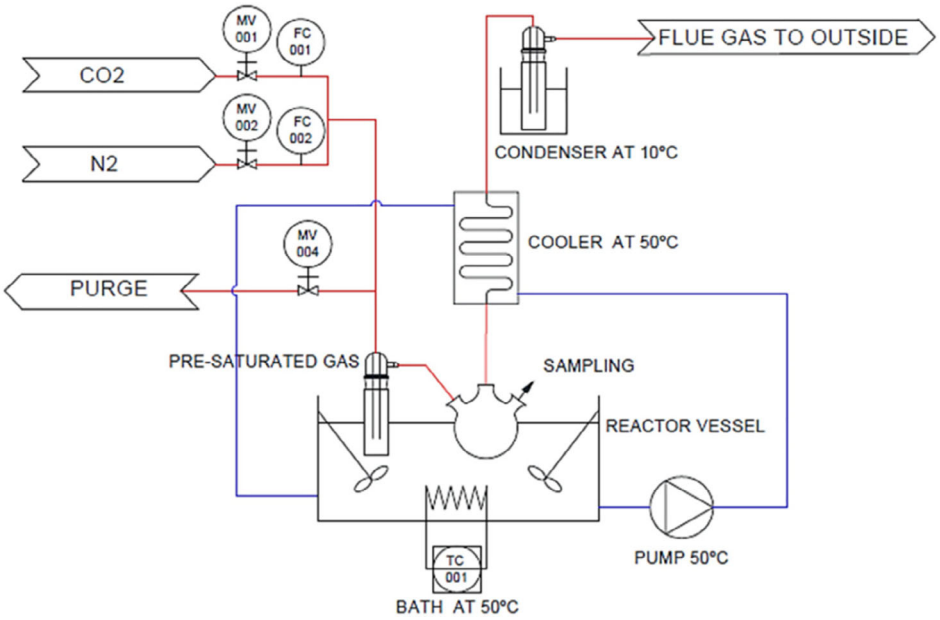

Figure 1. A flow diagram of the laboratory-scale semi-batch rig designed for the absorption performance evaluation of solvents under partial oxy-combustion conditions.

The absorption performances of the solvents tested in this work were evaluated from both the liquid and the gas phase. The CO_2 absorption experiments were carried out at different CO_2 concentrations of the flue gas, from post-combustion conditions (15%v/v CO_2) to partial oxy-combustion conditions, ≤60%v/v CO_2. Higher values of CO_2 concentration are not economically feasible for CO_2 capture applications, in which a full oxy-fuel combustion process is highly recommended.[5,7]

The absorption performance from the gas phase was analyzed by determining the CO_2 absorption rate through the experiments. These were determined continuously using measurements of the CO_2 concentration in the exhaust gas, using the expression indicated in Eqn (10)[27]:

$$R\,(\text{mL CO}_2\text{ per min}) = Q_{fg}\frac{[CO_2]_{IN}-[CO_2]_{OUT}}{1-[CO_2]_{OUT}} \qquad (10)$$

The CO_2 absorption performance from the liquid phase was evaluated using 1-mL liquid samples that were withdrawn through the tests. A total organic carbon (TOC) analyzer (Shimadzu model TOC-V CSH equipped with an auto-sampler model ASI-V) was chosen for the CO_2 loading determinations. According to Dinca *et al.*,[28] TOC is one of the most appropriate methods for CO_2 loading determinations because it is less susceptible to errors than other methods and exhibits an adequate period of time for sampling. The TOC equipment was calibrated following the analytical procedure reported in the standard test method UNE-EN 1484: 1998 and also described by Chen.[29]

The response to a general first-order dynamics system was used to adjust the CO2 loading evolution in the liquid phase during the experiments,[30] as seen in Eqn (11):

$$\alpha(t) = \alpha^{*}\left(1-e^{-t/\tau}\right) \qquad (11)$$

In Eqn (11), the characteristic time (τ) is an approximation of the mean average time of the absorption process of each experiment. According to Lin and Wong,[30] the ratio α:τ might approximately represent the average absorption rate from the liquid phase and it could be useful for further comparison of the CO_2 absorption performance of solvents under similar operating conditions.

RESULTS

The results and main conclusions extracted from this work are described in detail below. The results section is divided into gas- and liquid-phase evaluation of the CO_2 absorption performance of each solvent.

Gas-phase evaluation

The CO_2 absorption rates were calculated from measurements of the CO_2 concentration in the flue gas at both the inlet and the exhaust of the reactor vessel along each experiment using Eqn (10). The results are given in the three plots from Fig. 2. The CO_2 absorption rates increased using higher CO_2 concentration in the flue gas. The presence of higher amounts of CO_2 in the flue gas enhanced the absorption process and hence the CO_2 absorption rates also were improved. It should be pointed out that the kinetic behaviour observed for sterically hindered amines differed from primary amines (MEA). MEA experienced and enhancement of the CO_2 absorption kinetic as the CO_2 concentration shifted from 20%v/v CO_2 to 40%v/v CO_2. The equilibrium was achieved faster in those experiments run at 40%v/v CO_2 and 60% v/v CO_2. Both lines represented in Fig. 1(c) cross the previous ones obtained from 15%v/v CO_2 and 20%v/v CO_2, respectively.

On the contrary, the curves plotted for experiments of the sterically hindered amines reported a similar behaviour for all of the experiments run at different CO_2 concentrations. Although the increase of the CO_2 in the flue gas enhanced the absorption performance for this kind of amine-based solvent, it had no influence on the CO_2 absorption rate trend observed in curves plotted in Fig. 2(a) and (b), which were unchanged at CO_2 concentrations >40%v/v CO_2. The presence of higher amounts of CO_2 in the flue gas over 20%v/v promoted its reaction with the solvent to form the zwitterion intermediate [Eqn (1)]. For primary amines, the zwitterion intermediate rapidly reacts to produce carbamate anions that lead to further enhancement

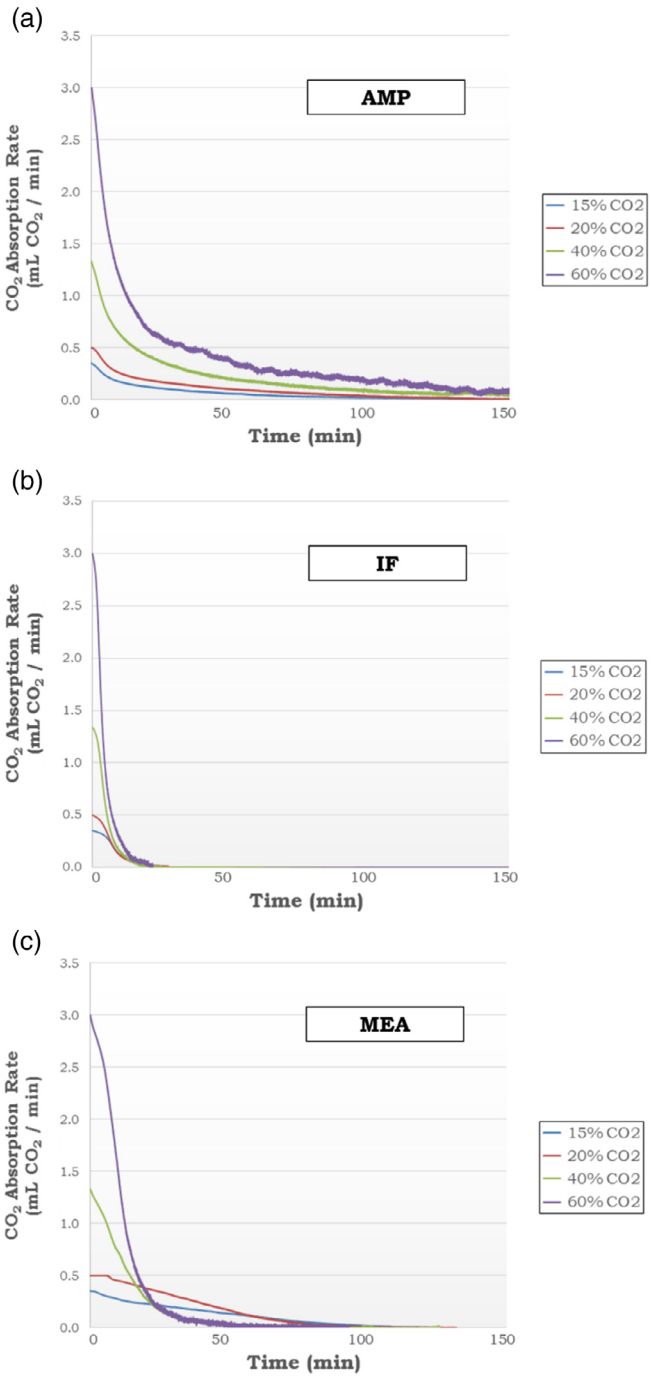

Figure 2. CO_2 absorption rate *versus* time for experiments performed at 50 °C, ambient pressure and 300 rpm with (a) AMP, (b) IF and (c) MEA * (adapted from Vega *et al.*[8]).

of the CO_2 absorption kinetics [Eqn (2)]. In the case of sterically hindered amines, the presence of more zwitterion intermediates due to the increase of the CO_2 concentration promotes CO_2 absorption but in bicarbonate form [Eqn (3)] which is slower than the carbamate reaction [Eqn (2)]. For this reason, an increase of the CO_2 concentration in the flue gas did not change the trend observed in Fig. 2(a) and (b) for sterically hindered amines. The absorption process occurred following the same pattern in all of the cases and the equilibrium was reached after 3 h regardless of the CO_2 concentration of the flue gas.

Table 2. Summary of the kinematic viscosity determinations

Solvent	Kinematic viscosity (cP) @ 25 °C	Kinematic viscosity (cP) @ 50 °C
MEA	2.4	1.3
AMP	1.7	1.2
IF	2.8	1.5

Liquid-phase evaluation

The kinematic viscosity was determined both at ambient and test temperatures before experiments were run. Table 2 summarizes the values obtained for each solvent listed in Table 1. The kinematic viscosity of MEA at 25 °C was the same reported by Weiland *et al.*[31]

The CO_2 loading (α) indicates the amount of CO_2 absorbed in the bulk liquid per mole of solvent dissolved in the aqueous solution. Figure 3 represents the evolution of CO_2 loading during the experiments for AMP and IF under variations of CO_2 concentration in the flue gas. The trends observed were similar to other work using similar rigs.[30]

First, AMP and IF achieved higher CO_2 loading at equilibrium compared with MEA for all of the CO_2 concentration tested in this work. AMP reached ≤1 mol CO_2 mol^{-1} solvent whereas IF achieved CO_2 loading >1.4 mol CO_2 mol^{-1} solvent at 60%v/v

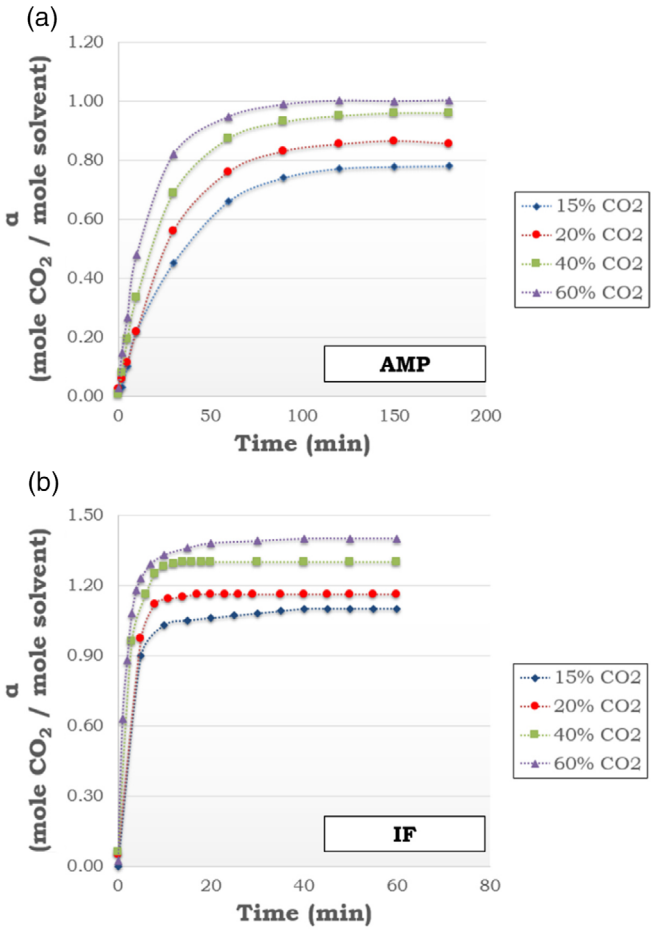

Figure 3. Evolution of the CO_2 loading for experiments performed at 50 °C, ambient pressure and 300 rpm with (a) AMP and (b) IF. The dotted lines provide a visual guideline of the trend.

Table 3. Adjustment of experimental model based on the response to a general first-order dynamics system for the CO_2 loading evolution

CO_2 concentration (%v/v)	Solvent	τ (s)	α^* (mole CO_2 mol^{-1} solvent)	Average absorption rate (α^*/τ) * 10^3
15	MEA	3108.27	0.535	0.172
	IF	215.97	1.101	5.099
	AMP	2443.96	0.803	0.329
20	MEA	1991.40	0.573	0.288
	IF	179.22	1.201	6.703
	AMP	2311.13	0.891	0.386
40	MEA	935.38	0.584	0.624
	IF	171.00	1.321	7.727
	AMP	1377.10	0.945	0.686
60	MEA	630.63	0.599	0.950
	IF	160.75	1.341	8.345
	AMP	975.29	1.002	1.027

CO_2 (Fig. 3). AMP and IF almost doubled the CO_2 loading of MEA: it could only reach a CO_2 loading slightly >0.5 mol CO_2 mol^{-1} solvent during the experiments run at CO_2 concentrations >15% v/v CO_2.[8]

AMP and IF experienced a 24.7% and 21.8% of increase in CO_2 loading at equilibrium as CO_2 varied from 15%v/v CO_2 to 60% v/v CO_2. Those values were higher than the increase observed for primary and secondary amines (fast kinetic solvents) such as MEA which reached 0.6 mol CO_2 mol^{-1} solvent at 60%v/v CO_2 (a 12% increase).[8]

The use of higher CO_2 concentration in the flue gas provided not only higher CO_2 loading of the solvent at the equilibrium, but also increased the CO_2 absorption rate for all of the solvents tested in this work (Fig. 3). In this respect, the characteristic time (τ) was closely related to the CO_2 absorption performance of the solvent. The values for τ determined in this work were summarized in Table 3. All of the solvents decreased τ under the presence of higher CO_2 concentration flue gas. MEA and AMP provided elevated characteristic times, ranging between 600 and 3200 s, in comparison with IF, which showed values ≈200 s and hence was considered the faster kinetics for the absorption process. The CO_2 absorption performance was similar to those observed for faster kinetic solvents.[8] Most of these solvents had very low characteristic time, below 1000 s. This fact confirmed that AMP and IF exhibited good kinetics even at low CO_2 concentration.

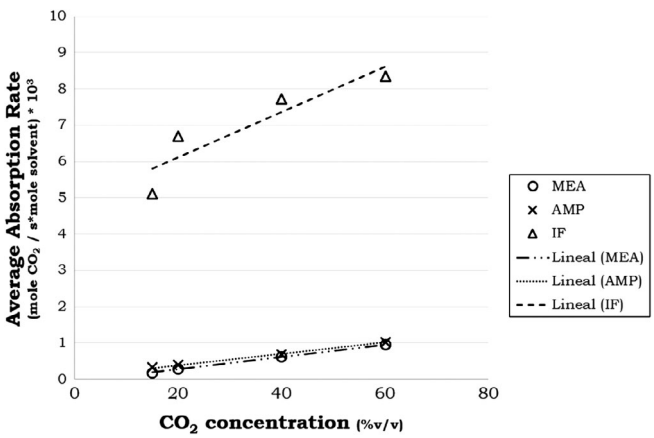

Figure 4. The average CO_2 absorption rates under variations on the CO_2 concentration of the flue gas for the solvents tested in this work. Experiments carried out at 50 °C, ambient pressure and 300 rpm.

The presence of higher CO_2 concentrations in the flue gas improved the CO_2 absorption process, producing significant reductions in characteristic times, ranging between 70% and 80%, compared with 15%v/v CO_2 experiments (Table 3). This behaviour is typical of fast kinetic solvents.[8]

Figure 4 represents the main average CO_2 absorption rate determined from the parameters obtained from the adjustment of the response to a general first-order step. In general, the use of higher CO_2 concentrations enhanced the CO_2 absorption rates for all the solvents: the absorption performance of AMP at low CO_2 concentrations was slightly better than that of MEA. The behaviour of AMP and MEA were identical at 60%v/v CO_2 from the main average absorption rate point of view; with respect to IF, it exhibited the fastest kinetics. The main average CO_2 absorption rate was up to eight-fold greater than that obtained from AMP and MEA, as seen in Fig. 4. IF also enhanced the CO_2 absorption performance in comparison with both AMP and MEA than AMP and MEA. The main average CO_2 absorption rate doubled – from $5*10^{-3}$ mol CO_2 / s*mol^{-1} solvent to $8.4*10^{-3}$ mol CO_2 / s*mol^{-1} solvent – as the CO_2 concentration shifted from 15%v/v CO_2 to 60%v/v CO_2 (Table 3).

CONCLUSIONS

This work evaluated the absorption performance of two sterically hindered amines under different CO_2 concentrations of flue gas which might be provided from partial oxy-combustion process regarding fossil-fuel power plants. In general, the presence of higher amounts of CO_2 in the flue gas enhanced CO_2 absorption and provided higher CO_2 absorption rates for all of the solvents tested in this work. It was observed that sterically hindered amines did not experience any changes in their absorption kinetic behaviour Under variations of the CO_2 concentrations mainly at values over 40%v/v CO_2, mainly at CO_2 concentrations over 40% v/v CO_2.

In addition, the evolution of CO_2 loading also exhibited higher values in the experiments using higher CO_2 concentration flue gas. AMP and IF achieved significant CO_2 loadings even at low CO_2 concentrations. They could be loaded up to 1 and 1.4 mol CO_2 mol^{-1} solvent, respectively, and doubled the CO_2 loading of MEA in most of the experiments.

The characteristic time (τ) decreased under the presence of higher CO_2 concentration flue gas, producing significant reductions (between 70% and 80%) of the characteristic time compared

with 15%v/v CO_2 experiments. MEA and AMP provided elevated characteristic times (>600 s), whereas the IF characteristic time was a lower order of magnitude (between 100 s and 200 s). This fact confirmed that AMP and IF exhibited favoured kinetics even at low CO_2 concentration in the flue gas. IF showed the faster kinetics for the absorption process. The kinetics rates observed using AMP were slightly higher than those for MEA, but lower than for IF which showed the fastest kinetic behaviour.

Therefore, AMP showed a similar absorption performance to MEA and it can be considered an excellent substitute for MEA for the CO_2 chemical absorption process associated with partial oxy-combustion technology, where there is elevated CO_2 concentration in the flue gas. IF exhibited fast kinetics and therefore it can be used as a promoter for new formulations applied to high CO_2 concentration flue gas processes.

ACKNOWLEDGEMENTS

This work was carried out with the financial support of the Ministry of Economy and Competitiveness of the Spanish Government (OXYSOLVENT Pro.; ref: CTM-2014-58573-R) co-financed by the European Development Research Fund (EDRF) from the European Union.

REFERENCES

1 DG for Climate Action, European Commission, Going Climate-Neutral by 2050. ISBN 978-92-76-02037-0 doi: https://doi.org/10.2834/02074 (2019).
2 De Vita A, Kielichowska I, Mandatowa P, Capros P. Technology Pathways in Decarbonisation Scenarios, ASSET Project Report. July 2018. Available: https://ec.europa.eu/energy/sites/ener/files/documents/2018_06_27_technology_pathways_-_finalreportmain2.pdf [30 October 2019].
3 https://www.co2.earth/. Consulting date 30 October 2019.
4 International Energy Agency, World Energy Outlook (2018). [30 October 2019]
5 Vega F, Cano M, Gallego LM, Camino S and Navarrete B, Evaluation of MEA 5M performance at different CO_2 concentrations of flue gas tested at a CO_2 capture lab-scale plant. *Energy Procedia* **114**: 6222–6228 (2017).
6 Laribi S, Dubois L, De Weireld G and Thomas D, Study of the post-combustion CO_2 capture process by absorption-regeneration using amine solvents applied to cement plant flue gases with high CO_2 contents. *Int J Greenhouse Gas Control* **90**:102799 (2019).
7 Cau G, Tola V, Ferrara F, Porcu A and Pettinau A, CO_2-free coal-fired power generation by partial oxy-fuel and post-combustion CO_2 capture: techno-economic analysis. *Fuel* **214**:423–435 (2018).
8 Vega F, Cano M, Camino S, Navarrete B and Camino JA, Evaluation of the absorption performance of amine-based solvents for CO_2 capture based on partial oxy-combustion approach. *Int J Greenhouse Gas Control* **73**:95–103 (2018).
9 Gouedard C, Picq D, Launay F and Carrette PL, Amine degradation in CO_2 capture. I. a review. *Int J Greenhouse Gas Control* **10**:244–270 (2012).
10 Vega F, Cano M, Sanna A, Infantes JM, Maroto Valer MM and Navarrete B, Oxidative degradation of a novel AMP/AEP blend designed for CO_2 capture based on partial oxy-combustion technology. *Chem Eng J* **350**:883–892 (2018).
11 Vega F, Camino S, Camino JA, Garrido J and Navarrete B, Partial oxy-combustion technology for energy efficient CO_2 capture process. *Appl Energy* **252**:113519 (2019).
12 Nwaoha C and Tontiwachwuthikul P, Carbon dioxide capture from pulp mill using 2-amino-2-methyl-1-propanol and monoethanolamine blend: techno-economic assessment of advanced process configuration. *Appl Energy* **250**:1202–1216 (2019).
13 Sartori G and Savage DW, Sterically hindered amines for carbon dioxide removal from gases. *Ind Eng Chem Fund* **22**:239–249 (1983).
14 Zhang P, Shi Y, Wei J, Zhao W and Ye Q, Regeneration of 2-amino-2-methyl-1-propanol used for carbondioxide absorption. *J Environ Sci* **20**:39–44 (2008).
15 Dash SD, Samanta AN and Bandyopadhyay SS, (vapour + liquid) equilibria (VLE) of CO_2 in aqueous solutions of 2-amino-2-methyl-1-propanol: new data and modelling using eNRTL-equation. *J Chem Thermodyn* **43**:1278–1285 (2011).
16 Vaidya PD and Kenig EY, CO_2-Alkanolamine reaction kinetics: a review of recent studies. *Chem Eng Technol* **30**:1467–1474 (2007).
17 Ramezani R, Mazinani S and Di Felice R, A comprehensive kinetic and thermodynamic study of CO_2 absorption in blends of monoethanolamine and potassium lysinate: experimental and modeling. *Chem Eng Sci* **206**:187–202 (2019).
18 Car A, Stropnik C, Yave W and Peinemann KV, Pebax/polyethylene glycol blend thin film composite membranes for CO_2 separation: performance with mixed gases. *Sep Purif Technol* **62**:110–117 (2008).
19 Park SH, Lee KB, Hyun JC and Kim SH, Correlation and prediction of the solubility of carbon dioxide in aqueous alkanolamine and mixed alkanolamine solutions. *Ind Eng Chem Res* **41**:1658–1665 (2002).
20 Dash SK, Samanta A, Samanta AN and Bandyopadhyay SS, Absorption of carbon dioxide in piperazine activated concentrated aqueous 2-amino-2-methyl-1-propanol solvent. *Chem Eng Sci* **66**:3223–3233 (2011).
21 Dash SK, Samanta AN and Bandyopadhyay SS, Solubility of carbon dioxide in aqueous solution of 2-amino-2-methyl-1-propanol and piperazine. *Fluid Phase Equilib* **307**:166–174 (2011).
22 Mondal MK, Balsora HK and Varshney P, Progress and trends in CO_2 capture/separation technologies: a review. *Energy* **46**:431–441 (2017).
23 Wai SK, Nwaoha C, Saiwan C, Idem R and Supap T, Absorption heat, solubility, absorption and desorption rates, cyclic capacity, heat duty, and absorption kinetic modeling of AMP–DETA blend for post–combustion CO_2 capture. *Sep Purif Technol* **194**:89–95 (2018).
24 Nwaoha C, Idem R, Supap T, Saiwan C, Tontiwachwuthikul P, Rongwong W *et al.*, Heat duty, heat of absorption, sensible heat and heat of vaporization of 2-amino-2-methyl-1-propanol (AMP), piperazine (PZ) and monoethanolamine (MEA) tri-solvent blend for carbon dioxide (CO_2) capture. *Chem Eng Sci* **170**:26–35 (2017).
25 Wang T and Jens KJ, Towards an understanding of the oxidative degradation pathways of AMP for post-combustion CO_2 capture. *Int J Greenhouse Gas Control* **37**:354–361 (2015).
26 Rochelle GT, Thermal degradation of amines for CO_2 capture. *Curr Opin Chem Eng* **1**:183–190 (2012).
27 Li J, You C, Chen L, Ye Y, Qi Z and Sundmacher K, Dynamics of CO_2 absorption and desorption processes in alkanolamine with cosolvent polyethylene glycol. *Ind Eng Chem Res* **51**:12081–12088 (2012).
28 Dinca C and Badea A, The parameters optimization for a CFBC pilot plant experimental study of post-combustion CO_2 capture by reactive absorption with MEA. *Int J Greenhouse Gas Control* **12**:269–279 (2013).
29 Chen, E., Carbon dioxide absorption into piperazine promoted potassium carbonate using structured packing. Thesis, University of Texas (2007).
30 Lin PH and Wong DSH, Carbon dioxide capture and regeneration with amine/alcohol/water blends. *Int J Greenhouse Gas Control* **26**:69–75 (2014).
31 Weiland RH, Dingman JC, Cronin DB and Browning GJ, Density and viscosity of some partially carbonated aqueous alkanolamine solutions and their blends. *J Chem Eng Data* **43**:378–382 (1998).

